ORIGINAL RESEARCH

FOXF1 Regulates Alveolar Epithelial Morphogenesis through Transcriptional Activation of Mesenchymal WNT5A

Abid A. Reza[1], Fatemeh Kohram[1], Hasan A. Reza[2], Timothy R. Kalin[3], Paranthaman S. Kannan[4], William J. Zacharias[4], and Vladimir V. Kalinichenko[1,2,4]

[1]Center for Lung Regeneration Medicine, [2]Division of Developmental Biology, and [4]Division of Pulmonary Biology, Cincinnati Children's Hospital Medical Center, Cincinnati, Ohio; and [3]University of Cincinnati, Cincinnati, Ohio

ORCID ID: 0000-0002-2643-0610 (W.J.Z.).

Abstract

Mutations in the *FOXF1* (forkhead box F1) gene, encoding the mesenchymal *FOX* (*forkhead box*) transcription factor, are linked to alveolar capillary dysplasia with misalignment of pulmonary veins (ACDMPV), a severe congenital disorder associated with the loss of alveolar capillaries and lung hypoplasia. Although proangiogenic functions of FOXF1 have been extensively studied, the role of FOXF1 in mesenchymal–epithelial signaling during lung development remains uncharacterized. Herein, we used murine lung organoids to demonstrate that the *S52F FOXF1* mutation (found in patients with ACDMPV) stimulates canonical WNT/β-catenin signaling in type 2 alveolar epithelial cells (AEC2s), leading to increased proliferation of AEC2s and decreased differentiation of AEC2s into type 1 alveolar epithelial cells (AEC1s). Alveolar organoids containing $Foxf1^{WT/S52F}$ lung fibroblasts and wild-type epithelial cells grew faster on Matrigel and exhibited AEC2 hyperplasia. AEC2 hyperplasia and loss of AEC1s were found in the lungs of $Foxf1^{WT/S52F}$ embryos, a mouse model of ACDMPV. Activation of canonical WNT/β-catenin signaling in AEC2s of lung organoids and $Foxf1^{WT/S52F}$ mice was associated with decreased expression of noncanonical WNT5A (Wnt family member 5A) ligand in lung fibroblasts. Mechanistically, FOXF1 directly activates the *Wnt5a* gene transcription through an evolutionarily conserved +6320/+6326 region located in the first intron of the *Wnt5a* gene. Site-directed mutagenesis of the +6320/+6326 region prevented the transcriptional activation of the *Wnt5a* enhancer by FOXF1. Treatment with exogenous WNT5A ligand inhibited the effects of the *S52F FOXF1* mutation on canonical WNT/β-catenin signaling in alveolar organoids, preventing aberrant AEC2 expansion and restoring differentiation of AEC1s. Activation of either FOXF1 or WNT5A may provide an attractive strategy to improve lung function in patients with ACDMPV.

Keywords: mesenchymal–epithelial signaling; lung development; alveolar capillary dysplasia; FOXF1 mutations; alveolar organoids

Mesenchymal–epithelial cell signaling plays a critical role in embryogenic and postnatal lung development (1–3). Lung morphogenesis in the mouse begins at 9.5 days after coitum (E9.5) and continues until Postnatal Day 30. Mesenchyme provides critical morphogenetic signals for developing respiratory epithelial cells that regulate epithelial lineage specification, differentiation, and branching lung morphogenesis (4). Among mesenchyme-derived morphogens are FGFs (fibroblast growth factors), WNTs, PDGF (platelet-derived growth factor), NOTCH, and TGF-β (transforming growth factor-β) (2, 4, 5). It is evident from published studies that canonical and noncanonical WNT signaling pathways play key roles in the proliferation, differentiation, and self-renewal of alveolar epithelial progenitor cells (3, 5, 6). WNT5A (Wnt family member 5A) is produced by lung mesenchyme, and $Wnt5a^{-/-}$ mice exhibit a truncation of the trachea and aberrant expansion of distal respiratory regions (7). In addition, increased proliferation and abnormal cell differentiation were observed in the epithelial

(Received in original form May 11, 2022; accepted in final form December 21, 2022)

Supported by National Heart, Lung, and Blood Institute grants HL141174, HL149631, and HL152973 (all to V.V.K.).

Author Contributions: V.V.K., A.A.R., and W.J.Z. designed the study. A.A.R., F.K., H.A.R., and P.S.K. performed experiments. W.J.Z. provided critical reagents. V.V.K., A.A.R., and T.R.K. wrote the manuscript with input from all authors.

Correspondence and requests for reprints should be addressed to Vladimir V. Kalinichenko, M.D., Ph.D., Cincinnati Children's Research Foundation, 3333 Burnet Avenue, MLC 7009, Cincinnati, OH 45229. E-mail: vladimir.kalinichenko@cchmc.org.

This article has a related editorial.

This article has a data supplement, which is accessible from this issue's table of contents at www.atsjournals.org.

Am J Respir Cell Mol Biol Vol 68, Iss 4, pp 430–443, April 2023

Originally Published in Press as DOI: 10.1165/rcmb.2022-0191OC on December 21, 2022
Internet address: www.atsjournals.org

Clinical Relevance

In the present study, we used murine lung organoids to demonstrate that the S52F FOXF1 (forkhead box F1) mutation in lung fibroblasts stimulates canonical WNT/β-catenin signaling in type 2 alveolar epithelial cells and inhibits their differentiation through regulation of WNT5A (Wnt family member 5A)–dependent mesenchymal–epithelial signaling. Activation of either FOXF1 or WNT5A may provide an attractive strategy to improve lung function in patients with neonatal lung diseases.

compartment of *Wnt5a*$^{-/-}$ mice, leading to inhibition of lung maturation (7). Conditional deletion of *CTNNB1* (*β-catenin*) driven by the *Sftpc* (surfactant protein C) promoter decreased the number of distal respiratory epithelial cells (8). In contrast, transgenic expression of constitutively active β-catenin in respiratory epithelial cells caused ectopic expression of proSP-C (pro–surfactant protein C) in conducting airways (9).

The transcription factor FOXF1 (forkhead box F1) is an evolutionarily conversed member of the FOX (forkhead box) family, which is critical for lung development in frogs, mice, and humans (2, 3, 10). Heterozygous copy-number variant deletions and point mutations in the *FOXF1* gene locus have been found in alveolar capillary dysplasia with misalignment of pulmonary veins (ACDMPV), a severe congenital lung disorder associated with defects in other organ systems (11, 12). The vast majority of infants with ACDMPV experience cyanosis, respiratory failure, and pulmonary hypertension in the first month after birth. Characteristic features of ACDMPV include paucity of alveolar capillaries, misalignment of pulmonary veins, impaired lobular development, and hyperplasia of type 2 alveolar epithelial cells (AEC2s). FOXF1 is expressed in mesenchyme-derived cells, including airway smooth muscle cells, lung endothelial cells, and fibroblasts (10, 13–16). In addition to its important role in lung angiogenesis (17–19), FOXF1 regulates various mesenchymal genes critical for mesenchymal–epithelial signaling during lung development (13). *Foxf1*$^{-/-}$ mice exhibit an embryonic lethal phenotype by E8.5 due to multiple developmental defects and the lack of vasculature in the yolk sac and allantois (20). Mice that are heterozygous for the *Foxf1* null allele (*Foxf1*$^{+/-}$) or the *S52F Foxf1* mutant allele (*Foxf1*$^{WT/S52F}$) exhibit alveolar capillary dysplasia and other developmental defects in the intestine, liver, and gallbladder (12, 21). Mesenchyme-specific inactivation of *Foxf1* using *Dermol-cre* causes embryonic lethality, lung hypoplasia, and severe abnormalities in the heart, liver, and esophagus (13). FOXF1 is required for lung angiogenesis by stimulating proangiogenic genes in endothelial cells (12, 22, 23). As multiorgan abnormalities indirectly influence lung morphogenesis in *Foxf1*-deficient mice, the direct effects of FOXF1 on mesenchymal–epithelial signaling remain poorly characterized.

In the past 10 years, several groups have developed different pulmonary organoid systems using lung epithelial progenitor populations such as basal cells, airway secretory club cells, AEC2s, and bronchioalveolar stem cells (24). Depending on the organoid type, some cultures require mesenchymal support. These three-dimensional multicellular lung organoids often recapitulate important aspects of some lung developmental processes and are useful to study mesenchymal–epithelial cross-talk during lung morphogenesis and regeneration (25). Lung organoids have been used to characterize progenitor cell populations in the lung, study molecular mechanisms of lung development and lung injury responses, and screen for potential drugs and small molecules for lung disease therapies (24). As *Foxf1* mutant mice exhibit severe vascular defects and multiorgan abnormalities (20, 21), lung organoids represent useful models to investigate the role of FOXF1 in mesenchymal–epithelial signaling. In this study, we used murine alveolar organoids generated from AEC2s with support from lung fibroblasts to determine the role of the *S52F Foxf1* mutation (identified in patients with ACDMPV) on canonical WNT/β-catenin signaling in AEC2s.

Methods

Ethics Statement

The corresponding author will provide data, analytic methods, and study materials on request to reproduce the results and replicate the procedures. All animal studies were approved by the Institutional Animal Care and Use Committee of the Cincinnati Children's Research Foundation.

Mouse Strains

CD1 mice were purchased from The Jackson Laboratory to isolate lung alveolar epithelial cells. The *Foxf1*$^{WT/S52F}$ mouse line was generated and maintained in a C57BL/6 × 129/J background as described (12, 26). The primers for genotyping of *Foxf1*$^{WT/S52F}$ mice were +77/+94 *Foxf1*, GGCGGCCAGGCCATGGAC; +112/+133 *Foxf1*, CACCAAGGCCAA-GAAGACCAAC; and +334/+313 *Foxf1*, GATGAAGCACTCGTTGAGCGAC (26). Eight- to 10-week-old *Foxf1*$^{WT/S52F}$, *Foxf1*$^{+/-}$ (21) mice, and wild-type (WT) littermates were used to isolate primary lung fibroblasts. For organoid studies, lung alveolar epithelial cells were isolated from WT mice (8–10 wk old). Lung tissue from *Foxf1*$^{WT/S52F}$ and WT mice was used for immunostaining and qRT-PCR of total lung RNA as described (27–30).

Generation of Alveolar Organoids and AEC2 Culture

Clonal alveolar organoids were generated using a previously described protocol (31). Briefly, lung fibroblasts were isolated from *Foxf1*$^{WT/S52F}$ and WT mice as previously described (31). For isolation of lung epithelial cells, single-cell suspension was prepared from mouse lung tissue using enzymatic digestion, and subsequently, this cell suspension was purified using immunomagnetic beads to isolate CD45$^-$ CD16/32$^-$ Ter119$^-$ CD90$^-$ CD31$^-$ NGFR$^-$ (nerve growth factor receptor) CD326$^+$ cells as described (31). For each well, 5×10^3 epithelial cells were mixed with 5×10^4 lung fibroblasts, and the cells were placed into a 1:1 mixture (90 μl) of SAGM medium (Lonza) and growth factor–reduced, phenol-free Matrigel (Corning). The mixture was plated on cell culture inserts (0.4 μm), which were then placed into a 24-well plate and allowed to solidify at 37°C. Next, SAGM medium was placed into the wells. ROCK (rho-associated coiled-coil containing protein kinase) inhibitor Y27632 (Sigma-Aldrich) was added with the medium only for the first 48 hours as described (31). Medium was replaced every 48 hours. After 21 days, the organoids were recovered and used for whole-mount immunostaining, preparation of paraffin-embedded blocks, or RNA isolation. For WNT5A treatment, the human/mouse recombinant WNT5A

ligand (R&D Systems) with a 50 ng/ml concentration was added to the medium for the total duration of the experiments. WNT5A blocking antibodies (R&D Systems) were used in a 500 ng/ml concentration to inhibit WNT5A in the organoid cultures. For the AEC2 culture, purified lung epithelial cells were isolated and placed into Matrigel without fibroblasts. Fibroblast culture medium was then added to the epithelial cells in a 1:1 ratio with SAGM medium.

Immunostaining

Immunostaining of paraffin-embedded sections and whole-mount immunostaining were used to visualize cells in lung organoids. For whole-mount immunostaining, organoids were recovered from the Matrigel using cell recovery solution (Corning), fixed in 4% paraformaldehyde (PFA), stained with antibodies (*see* Table E1 in the data supplement), and mounted on microscope slides in fructose–glycerol clearing solution. For staining of paraffin-embedded sections, organoids with Matrigel were fixed in 4% PFA, embedded in HistoGel (Richard-Allan), dehydrated, embedded in paraffin, and sectioned. To generate tissue blocks from mouse embryonic lungs, lungs were harvested from the WT and *Foxf1*$^{WT/S52F}$ 18.5 days after coitum (E18.5) embryos and embedded in paraffin or used to prepare optimal cutting temperature (OCT) frozen blocks. Paraffin-embedded and frozen sections were immunostained with antibodies listed in Table E1 as described (32–34). The slides were counterstained with DAPI (Vector Laboratories) to visualize the cell nuclei. Two-dimensional and volumetric (Z-stack) images were acquired as described (35, 36) using the confocal Nikon A1 microscope.

RNAScope Assay and Cell Proliferation (5-Ethynyl-2′-Deoxyuridine) Assay

Frozen mouse embryo lung sections were stained using the RNAScope Multiplex Fluorescent Reagent Kit (version 2) (Advanced Cell Diagnostics) and Opal Fluorophore reagents (Advanced Cell Diagnostics) following manufacturer recommendations as described (22). The following riboprobes from Advanced Cell Diagnostics were used: Mm-Wnt5a (316791) and Mm-Vim-C2 (457961-C2).

For the organoid-based proliferation assay, 5-ethynyl-2′-deoxyuridine (EdU) solution from the Click-iT Plus EdU Cell Proliferation Kit (Invitrogen) was added to the organoid culture 48 hours before organoid harvest. The manufacturer-recommended protocol was used for EdU staining. For the fibroblast proliferation assay, EdU solution was added to the cell culture 6 hours after cell seeding. Cells were fixed in 4% PFA and stained for EdU.

mRNA Isolation, qRT-PCR, and ELISA

Cells were recovered from Matrigel after treating the organoids with Dispase (Corning) and 0.05% trypsin–EDTA (Gibco). mRNA was isolated from lung organoids, mouse lung tissue, or purified lung fibroblasts using the RNeasy Plus Mini Kit or the RNeasy Micro Kit (Qiagen). qRT-PCR analysis was performed using the StepOnePlus or QuantStudio 3 Real-Time PCR system (Applied Biosystems) as described (37, 38). TaqMan primers (Thermo Fisher Scientific) (*see* Table E2) were used to amplify cDNA. Concentrations of WNT5A protein in conditioned media from cultured fibroblasts were measured using the ELISA WNT5A kit (Cusabio) according to manufacturer recommendations.

Motif Analysis, Chromatin Immunoprecipitation-Quantitative PCR, and Dual-Luciferase Assay

Motif analysis of FOXF1-binding sites in mouse *Wnt5a* gene locus was conducted using a published chromatin Immunoprecipitation sequencing (ChIP-seq) data set generated from mouse WT E18.5 lungs (accession number GSE77951) (39). Data analysis was performed using the SciDAP platform (previously BioWardrobe) and the University of California, Santa Cruz, Genome Browser as described (40). Chromatin Immunoprecipitation-Quantitative PCR (ChIP-qPCR) was performed using the High Sensitivity ChIP Kit (Abcam). Briefly, whole chromatin was prepared from cultured lung fibroblasts and then crosslinked and sonicated to an optimal size of 300 bp (confirmed using gel electrophoresis). Chromatin was used for immunoprecipitation (IP) with either FOXF1 antibodies or IgG1 isotype control (*see* Table E1). DNA fragments were amplified using custom primers listed in Table E3. Fold enrichment was normalized to IP from IgG controls.

The FOXF1–luciferase (LUC) reporter plasmid contained six multimerized FOXF1-binding sites placed upstream of the minimal cytomegalovirus (CMV) promoter driving LUC expression. The FOXF1–LUC reporter was used as a readout of FOXF1 transcriptional activity as described (41). The *Wnt5a* enhancer was cloned into a pGL4.23–LUC reporter plasmid (Promega) inside the multiple cloning site. A site-directed mutagenesis kit (New England Biolabs) was used to disrupt the FOXF1-binding sites and generate FOXF1 mutant constructs. Dual-LUC assay (Promega) was performed as described (14, 41, 42) in human embryonic kidney 293T cells, which do not express endogenous FOXF1. Exogenous FOXF1 was expressed in human embryonic kidney 293T cells using the CMV–*Foxf1* expression plasmid. A CMV–empty vector was used as a control, and CMV–Renilla was used as an internal control to normalize the transfection efficiency (14).

Statistical Analysis

All statistical analyses were performed using Prism 9 software (GraphPad Software). An unpaired two-tailed Student's *t* test was used to compare two experimental groups. For experiments with more than two groups, one-way ANOVA was used. P values ≤ 0.05 were considered to indicate statistical significance. All values are expressed as mean ± SEM.

Results

The *S52F Foxf1* Mutation in Lung Fibroblasts Accelerates the Growth of Lung Alveolar Organoids and Alters the Differentiation of Respiratory Epithelial Cells

To examine the effect of the *S52F FOXF1* mutation (found in patients with ACDMPV) on mesenchymal–epithelial signaling, we generated lung organoids using primary lung fibroblasts from *Foxf1*$^{WT/S52F}$ mice and purified CD326^{+} lung epithelial cells from WT mice (Figures 1A and 1B and E1A–E1C). FOXF1 activity in *Foxf1*$^{WT/S52F}$ fibroblasts was examined before organoid formation. Although *Foxf1* mRNA expression was similar in *Foxf1*$^{WT/S52F}$ mutant fibroblasts compared with controls (*see* Figure E1D), FOXF1 functional activity was lower, as demonstrated by the LUC reporter assay using FOXF1-specific LUC reporter plasmid (Figure 1A). As FOXF1 stimulates *Cdh2* (cadherin 2) but inhibits *Cdh11* gene transcription in lung fibroblasts (14), we examined *Cdh2* and *Cdh11* mRNAs in *Foxf1*$^{WT/S52F}$ fibroblasts. Consistent with decreased FOXF1 activity, *Cdh2* mRNA

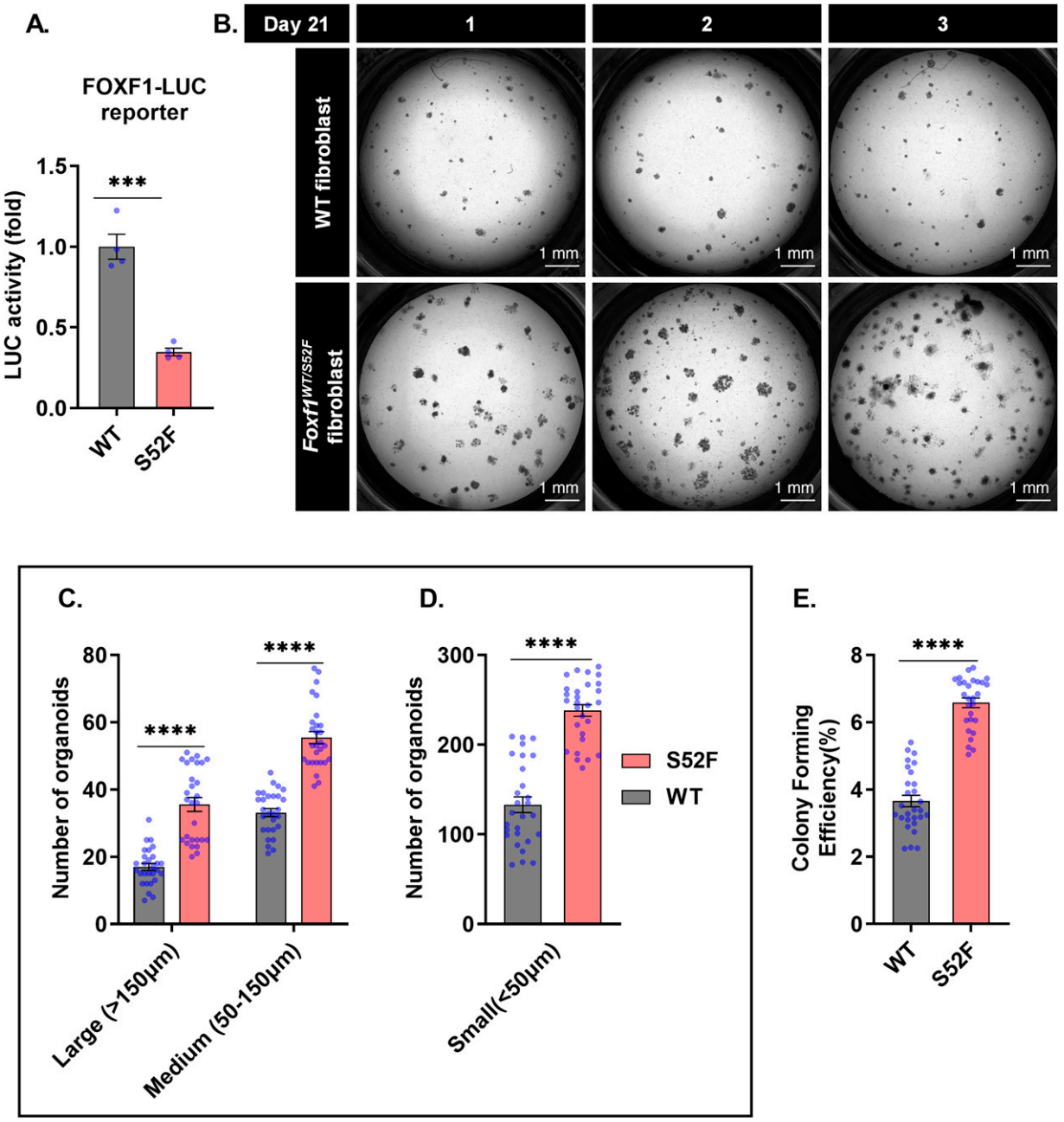

Figure 1. The *S52F Foxf1* (forkhead box F1) mutation in lung fibroblasts increases the number and size of lung organoids. (*A*) LUC assay shows that *Foxf1*$^{WT/S52F}$ fibroblasts exhibit decreased FOXF1 transcriptional activity compared with wild-type (WT) lung fibroblasts (control). Lung fibroblasts were isolated from either *Foxf1*$^{WT/S52F}$ or WT mice ($n = 4$ mice in each group). (*B*) The use of *Foxf1*$^{WT/S52F}$ fibroblasts and WT epithelial cell results in increased number and size of organoids. Images were taken 21 days after the initiation of organoid culture on Matrigel. Scale bars, 1 mm. (*C* and *D*) The number of large (>150 μm), medium (50–150 μm), and small (<50 μm) organoids was increased after coculture of WT epithelial cells with *Foxf1*$^{WT/S52F}$ fibroblasts ($n = 28$ wells). (*E*) The colony-forming assay shows that *Foxf1*$^{WT/S52F}$ fibroblasts are more efficient than WT fibroblasts to form organoids with WT epithelial cells ($n = 28$ wells). ***$P < 0.001$ and ****$P < 0.0001$. LUC = luciferase.

was lower and Cdh11 mRNA was higher in *Foxf1*$^{WT/S52F}$ cells compared with WT controls (*see* Figure E1D). We also tested the purity of lung fibroblasts by examining the mRNAs of various cell markers. Lung fibroblasts from both *Foxf1*$^{WT/S52F}$ and WT mice expressed fibroblasts cell markers such as *Des* (desmin) and *Vim* (vimentin) (*see* Figure E2A) but were negative for markers of other respiratory cell types, including hematopoietic (*see* Figure E2B), epithelial (*see* Figure E2C), and endothelial (*see* Figure E2D) cells. The *Foxf1*$^{WT/S52F}$ mutation did not influence the proliferation of lung fibroblasts in cell culture conditions (*see* Figures E3A–E3C).

A comparison of lung organoids with *Foxf1*$^{WT/S52F}$ and WT fibroblasts demonstrated that the number and size of organoids containing *Foxf1*$^{WT/S52F}$ fibroblasts were higher (Figures 1B–1D).

Consistent with an increased number of *Foxf1*$^{WT/S52F}$ organoids, the colony-forming efficiency of the *Foxf1*$^{WT/S52F}$ organoids was increased compared with controls (Figure 1E). On the basis of average diameter, the organoids were subdivided into small (<50 μm), medium (50–150 μm), and large (>150 μm). *Foxf1*$^{WT/S52F}$ fibroblasts increased the number of lung organoids in all size categories (Figures 1C and 1D). The *Foxf1* haploinsufficiency had similar effects as the *Foxf1*$^{WT/S52F}$ mutation because *Foxf1*$^{+/-}$ fibroblasts increased the number and size of lung organoids (*see* Figures E4A–E4C) and increased the colony-forming efficiency in organoid three-dimensional cultures (*see* Figure E4D). The presence of lung fibroblasts was required for the formation of organoids because the addition of fibroblast culture media to lung epithelial cells failed to stimulate the organoid formation (*see* Figure E5A) and maintain the expression of proSP-C (*see* Figure E5B).

Whole-mount immunostaining of lung organoids with AEC2 marker proSP-C and type 1 alveolar epithelial cell (AEC1) marker RAGE (receptor for advanced glycation end products) revealed the presence of AEC1s and AEC2s in organoids formed by either WT or *Foxf1*$^{WT/S52F}$ fibroblasts (Figure 2A). The organoids did not express CCSP (club cell secretory protein), a marker of airway epithelial club cells (*see* Figure E6), or MUC5AC, a marker of mucus-producing goblet cells (*see* Figure E7A). α-SMA^{+} (α-smooth muscle actin) myofibroblasts were often observed in the outer layers of organoids (*see* Figure E6). Apoptotic cells were undetectable in the *Foxf1*$^{WT/S52F}$ and WT organoids, as shown by immunostaining for activated caspase-3 (*see* Figure E7B). Lung organoids grown in the presence of *Foxf1*$^{WT/S52F}$ fibroblasts had a higher percentage of AEC2s than WT organoids (Figure 2B). In contrast, the percentage of AEC1s in *Foxf1*$^{WT/S52F}$ organoids was lower (Figure 2B). These results are consistent with qRT-PCR analysis demonstrating that AEC1 mRNAs (*Aqp5* [aquaporin 5], *Ager* [advanced glycosylation end product-specific receptor]) were decreased, whereas AEC2 mRNA (*Sftpc*) was increased in *Foxf1*$^{WT/S52F}$ organoids compared with WT organoids (Figure 2C). RAGE and proSP-C did not colocalize in the *Foxf1*$^{WT/S52F}$ and WT organoids in our experimental conditions (*see* Figure E8). Thus, the *S52F Foxf1* mutation in lung fibroblasts alters the differentiation of alveolar epithelial cells and increases the size and number of alveolar organoids.

The *S52F Foxf1* Mutation in Lung Fibroblasts Increases Canonical WNT/β-Catenin Signaling in AEC2s of Lung Organoids

To determine which cells were responsible for the increased growth of lung alveolar organoids containing *Foxf1*$^{WT/S52F}$ fibroblasts, we stained the organoids for cyclin D1, a marker of proliferative cells (33). Whole-mount immunostaining for cyclin D1 and proSP-C demonstrated that alveolar organoids with *Foxf1*$^{WT/S52F}$ fibroblasts had an increased number of AEC2s undergoing the cell cycle (Figures 3A and 3B). *Ccnd1* (cyclin D1) mRNA was increased in *Foxf1*$^{WT/S52F}$ lung organoids, as demonstrated by qRT-PCR (Figure 3C). There were no proliferative cells among AEC1s, as shown by immunostaining for cyclin D1 and RAGE (Figures 3A and 3B)

As canonical WNT/β-catenin signaling increases epithelial proliferation and cyclin D1 is a downstream target of this signaling pathway (2, 33), we stained lung organoids for activated phospho-β-catenin (Figure 4A). The percentage of AEC2s with activated nuclear β-catenin was increased in lung organoids containing *Foxf1*$^{WT/S52F}$ fibroblasts (Figure 4B). Activated β-catenin was not detected in AEC1s in either WT or *Foxf1*$^{WT/S52F}$ organoids (Figures 4A and 4B). Although *Ctnnb1* mRNA did not change in the *Foxf1*$^{WT/S52F}$ organoids, mRNAs of WNT/β-catenin target genes *Fzd1* (frizzled class receptor 1) and *Axin2* (axin 2) were higher (Figure 4C). This finding was consistent with increased nuclear translocation of activated phospho-β-catenin in AEC2s (Figures 4A and 4B). Activated phospho-β-catenin colocalized with EdU in cycling AEC2s (*see* Figure E9). Thus, the *S52F Foxf1* mutation in lung fibroblasts increases canonical WNT/β-catenin signaling and cellular proliferation in AEC2s but not in AEC1s.

The *S52F Foxf1* Mutation Alters the Differentiation of Alveolar Epithelial Cells during Lung Development

As the *S52F Foxf1* mutation in lung fibroblasts increases canonical WNT/β-catenin signaling and alters differentiation of alveolar epithelial cells in lung organoids, we used lungs of *Foxf1*$^{WT/S52F}$ and WT E18.5 embryos to establish the biological relevance of our organoid studies to lung development in the mouse. Immunostaining of lung tissue sections for proSP-C, HOPX, and T1α revealed that *Foxf1*$^{WT/S52F}$ lungs have an increased proportion of AEC2s among alveolar epithelial cells compared with lungs of WT littermates (Figures 5A and 5B). In contrast, the ratio of AEC1s, labeled by HOPX and T1α, was reduced (Figures 5A and 5B). Consistent with the altered AEC2:AEC1 ratio in *Foxf1*$^{WT/S52F}$ mutant lungs, *Sftpc* mRNA in total lung lysate was increased, whereas mRNAs of *Ager* and *Aqp5* decreased (Figure 5C). Furthermore, *Foxf1*$^{WT/S52F}$ lungs had a higher percentage of AEC2s with nuclear expression of activated phospho-β-catenin (Figures 5D and 5E), supporting increased canonical WNT/β-catenin signaling in AEC2s of *Foxf1*$^{WT/S52F}$ mutant lungs. Finally, *Foxf1*$^{WT/S52F}$ mice exhibited increased proliferation of AEC2s as demonstrated by immunostaining for cyclin D1 and proSP-C (*see* Figures E10A and E10B) and increased expression of canonical WNT target gene Axin2 (Figure 5F). Thus, consistent with our organoid studies, the *S52F Foxf1* mutation increases canonical WNT/β-catenin signaling in developing AEC2s, causing increased AEC2 proliferation and altering the normal differentiation of alveolar epithelial cells during lung development.

FOXF1 Directly Activates *Wnt5a* Gene Expression in Lung Fibroblasts

Published studies have demonstrated that WNT5A, a noncanonical WNT ligand produced by lung fibroblasts, inhibits canonical WNT/β-catenin signaling in AEC2s of lung organoids (43) and *in vivo* (44). Therefore, we tested whether FOXF1 regulates the expression of WNT5A. Using FOXF1 ChIP sequencing data sets from mouse E18.5 lungs (39), we identified the FOXF1-binding region in the first intron of the mouse *Wnt5a* gene (Figure 6A). The FOXF1-binding region exhibited activating histone marks H3K3me1 and H3K4me3 but was negative for the H3K9me3 mark, which is consistent with enhancer properties (Figure 6A). To validate the FOXF1 binding to the *Wnt5a* enhancer, FOXF1 ChIP-qPCR was performed using primary lung fibroblasts. FOXF1 is directly bound to the *Wnt5a* intronic enhancer, and the FOXF1 binding was decreased in *Foxf1*$^{WT/S52F}$ lung fibroblasts compared with WT lung fibroblasts (Figure 6B). The *Wnt5a* enhancer is evolutionarily conserved

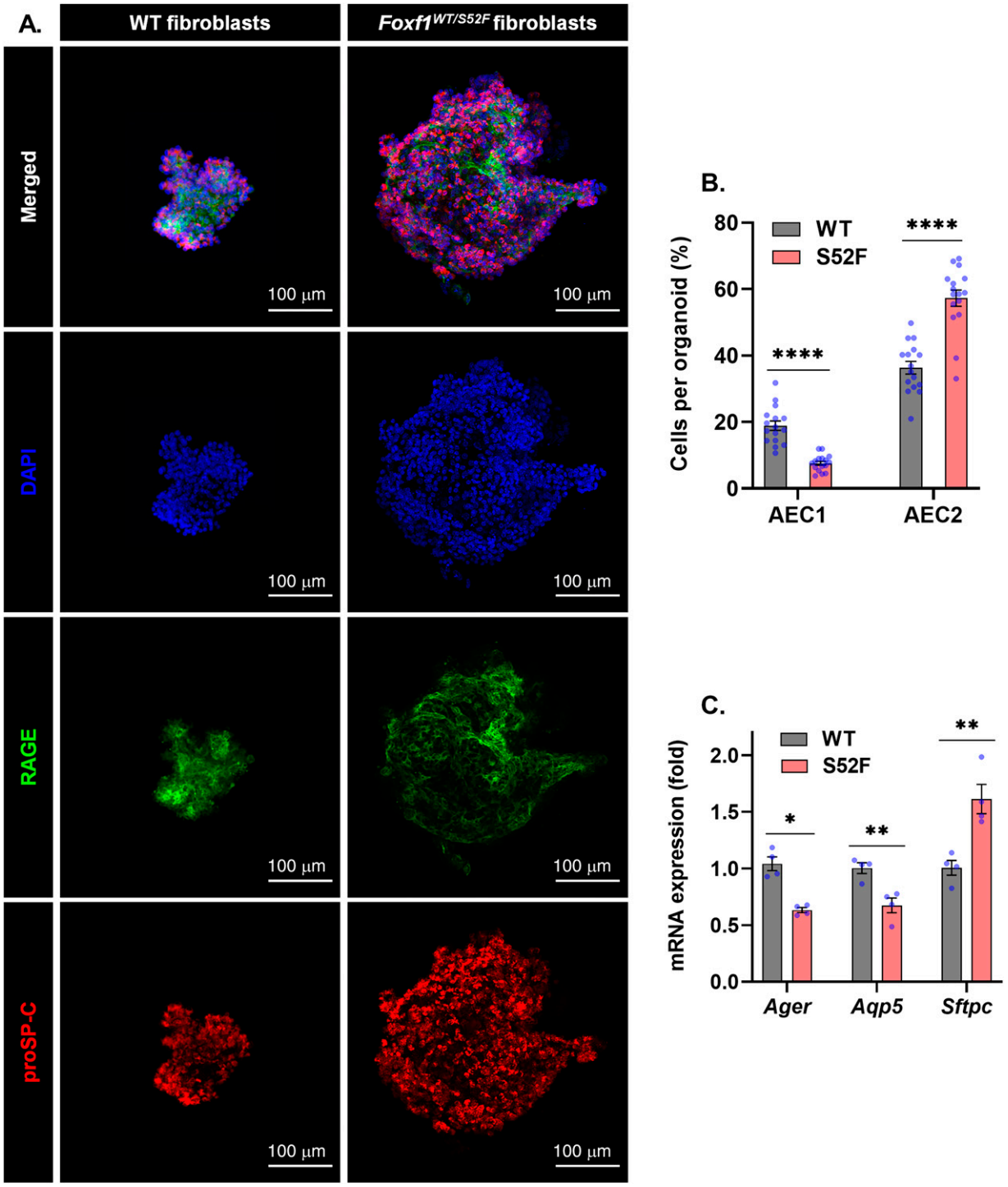

Figure 2. The *S52F Foxf1* mutation in lung fibroblasts alters the cellular composition of alveolar organoids. (*A*) Confocal images of alveolar organoids identify type 1 alveolar epithelial cells (AEC1s) (RAGE [receptor for advanced glycation end products], green) and type 2 alveolar epithelial cells (AEC2s) (proSP-C [pro–surfactant protein C], red). Images were obtained after whole-mount staining of lung organoids using antibodies specific to RAGE and proSP-C. Cell nuclei were counterstained with DAPI (blue). Scale bars, 100 μm. (*B*) Quantification of alveolar epithelial cells in organoids reveals that organoids with *Foxf1*$^{WT/S52F}$ fibroblasts have increased percentages of AEC2s but decreased percentages of AEC1s. AEC2s and AEC1s were counted using high-magnification images from proSP-C–stained and RAGE-stained organoids ($n = 16$). (*C*) qRT-PCR shows decreased *Ager* and *Aqp5* mRNAs and increased *Sftpc* mRNA in lung organoids containing *Foxf1*$^{WT/S52F}$ fibroblasts ($n = 4$). mRNA concentrations were normalized to *Actb* mRNA. *$P < 0.05$, **$P < 0.01$, and ****$P < 0.0001$. *Actb* = actin beta; *Ager* = advanced glycosylation end product-specific receptor; *Aqp5* = aquaporin 5; *Sftpc* = surfactant protein C.

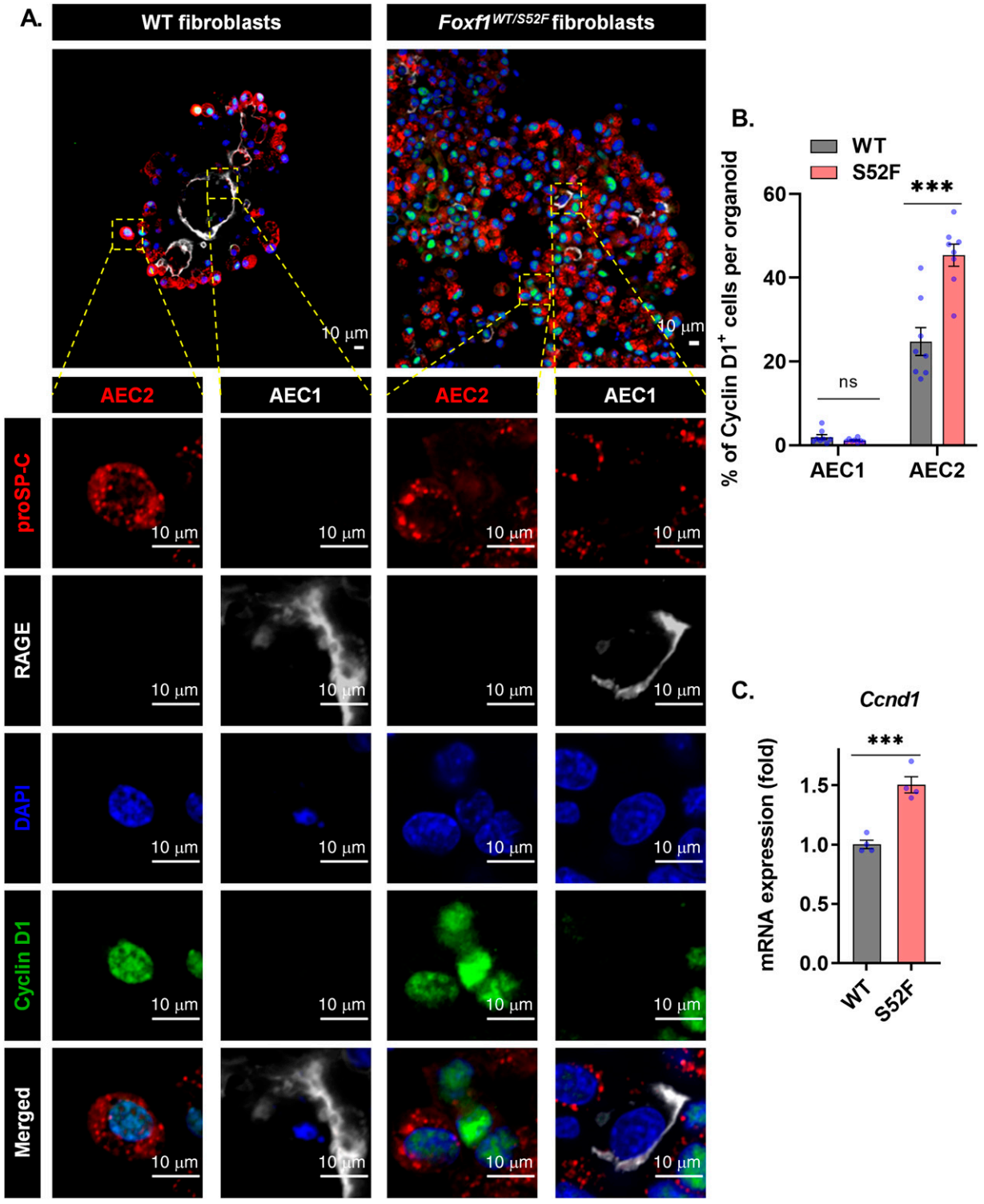

Figure 3. Lung organoids with *Foxf1*$^{WT/S52F}$ fibroblasts exhibit an increased percentage of proliferative AEC2s. (*A*) Whole-mount immunostaining of lung organoids for cyclin D1 (green), proSP-C (red), and RAGE (white) shows nuclear cyclin D1 expression in AEC2s but not in AEC1s. Scale bars, 10 μm. (*B*) The percentage of cyclin D1–positive AEC2s is increased in organoids containing *Foxf1*$^{WT/S52F}$ fibroblasts. Cyclin D1–positive AEC2s and AEC1s were counted using high-magnification images from organoids stained for cyclin D1, proSP-C, and RAGE ($n = 8$). (*C*) qRT-PCR shows that *Ccnd1* mRNA is increased in organoids containing *Foxf1*$^{WT/S52F}$ fibroblasts ($n = 4$). mRNA concentrations were normalized to A*ctb* mRNA. ***$P < 0.001$. *Ccnd1* = cyclin D1; ns = not significant.

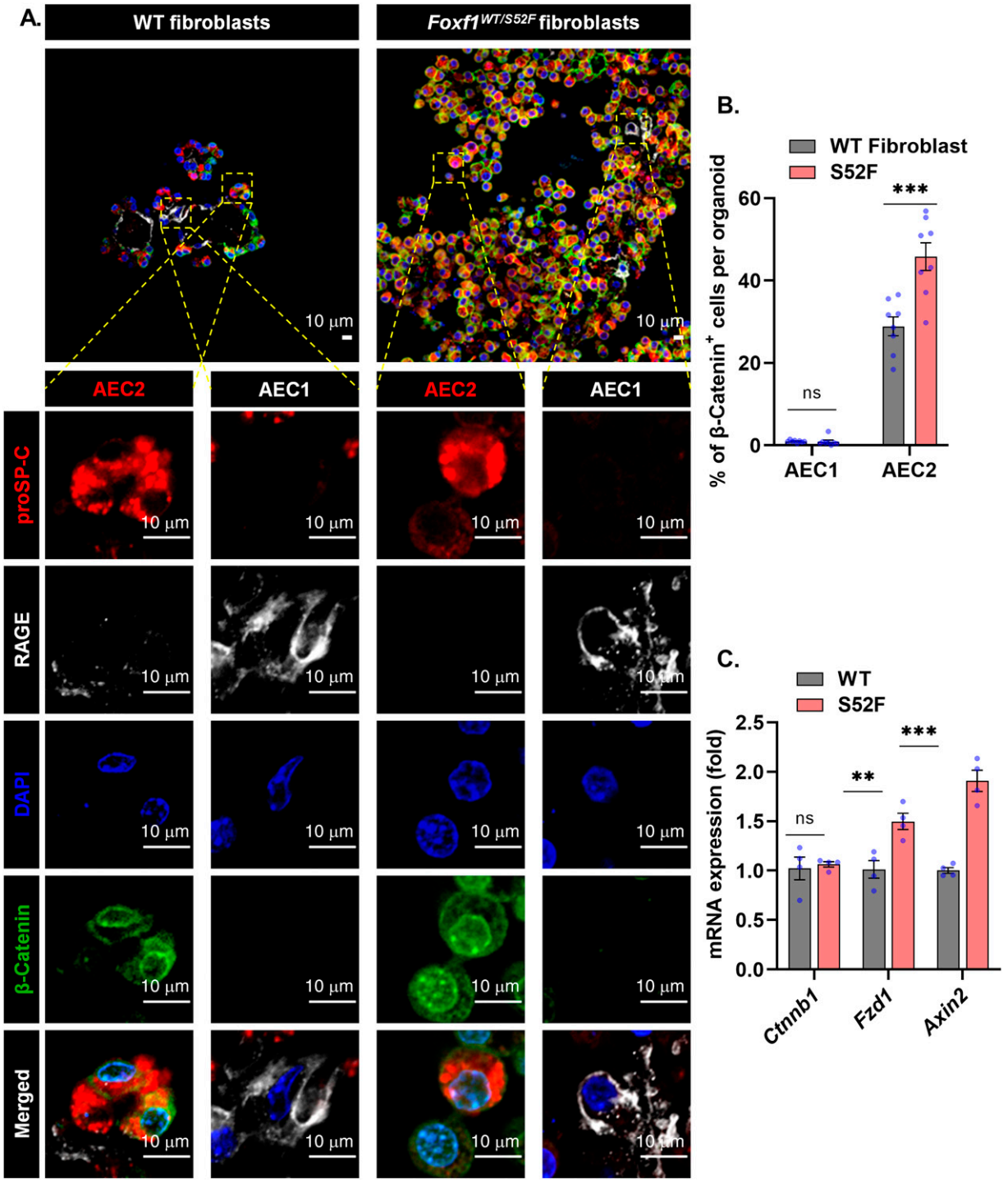

Figure 4. The *S52F Foxf1* mutation increases the percentage of AEC2s with nuclear expression of activated β-catenin. (*A*) Whole-mount immunostaining of lung organoids shows the presence of activated phospho-β-catenin (green) in proSP-C$^+$ AEC2s (red) but not in RAGE$^+$ AEC1s (white). Cell nuclei were counterstained with DAPI (blue). Scale bars, 10 μm. (*B*) The percentage of AEC2s with nuclear β-catenin is increased in organoids containing *Foxf1*$^{WT/S52F}$ fibroblasts ($n = 8$). (*C*) qRT-PCR shows that *Ctnnb1* mRNA is unchanged, but *Fzd1* and *Axin2* mRNAs are increased in *Foxf1*$^{WT/S52F}$ lung organoids compared with WT controls ($n = 4$). mRNA concentrations were normalized to A*ctb* mRNA. $^{**}P < 0.01$ and $^{***}P < 0.001$. *Axin2* = axin 2; *Ctnnb1* = β-catenin; *Fzd1* = frizzled class receptor 1.

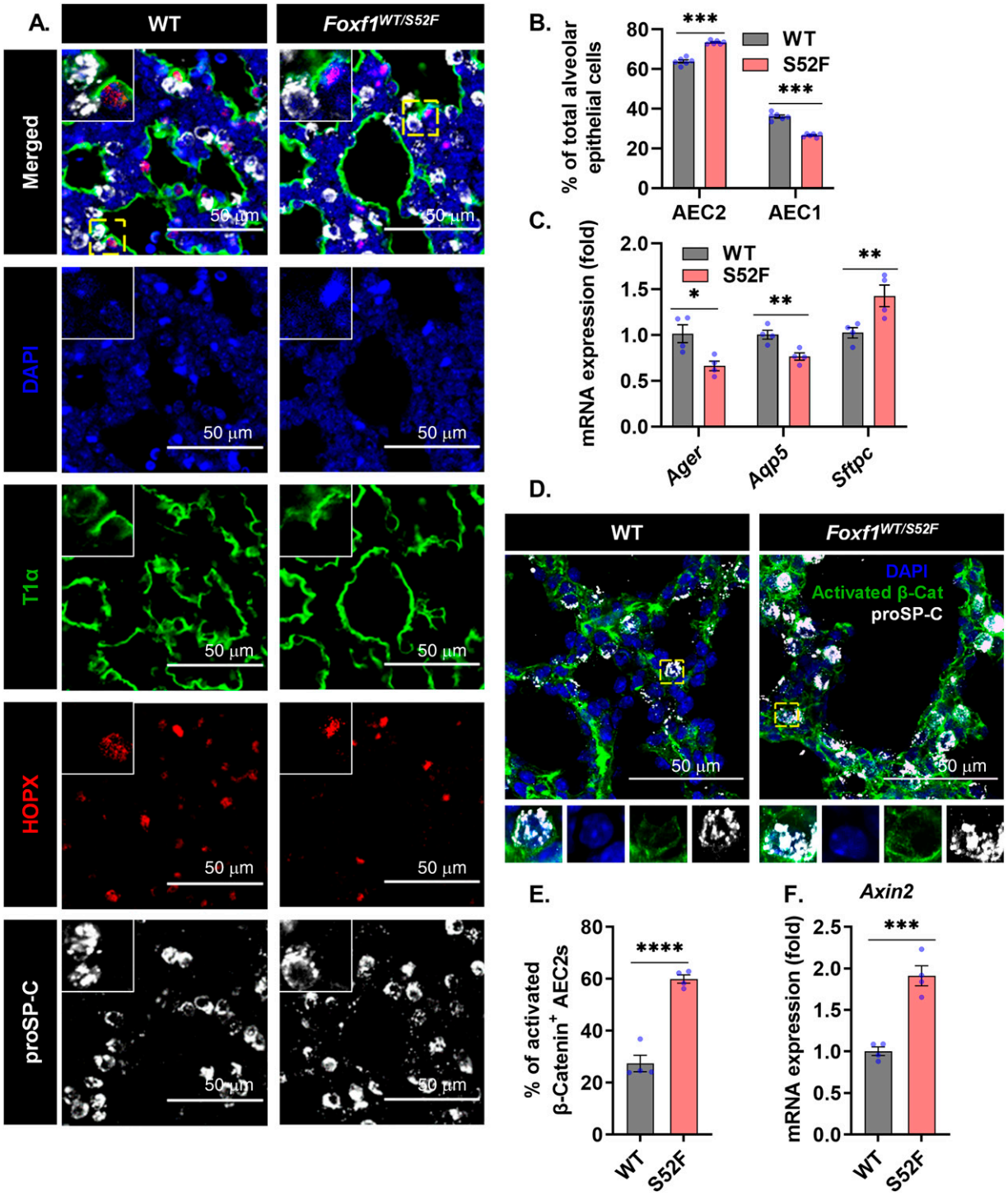

Figure 5. The *S52F Foxf1* mutation disrupts epithelial differentiation during lung development. (*A*) Images of lung sections from WT and *Foxf1*$^{WT/S52F}$ E18.5 lung embryos were stained for AEC1 markers (HOPX and T1α) and AEC2 marker (proSP-C). Scale bars, 50 μm. (*B*) The percentage of AEC2s among total alveolar epithelial cells is increased in *Foxf1*$^{WT/S52F}$ lungs compared with WT lungs ($n = 6$ mice in each group). (*C*) qRT-PCR shows that mRNA expression of *Sftpc* is increased, whereas *Ager* and *Aqp5* mRNAs are decreased in *Foxf1*$^{WT/S52F}$ lungs ($n = 4$ lungs in each group). mRNA concentrations were normalized to *Actb* mRNA. (*D* and *E*) Immunostaining for proSP-C (white) and activated phospho-β-catenin (green) shows that the number of AEC2s with nuclear expression of phospho-β-catenin among total AEC2s is increased in *Foxf1*$^{WT/S52F}$ lungs compared with WT controls ($n = 4$). Cell nuclei were counterstained with DAPI (blue). Scale bars, 50 μm. (*F*) qRT-PCR shows that mRNA expression of *Axin2* is increased in *Foxf1*$^{WT/S52F}$ lungs compared with WT lungs ($n = 4$ mice in each group). mRNA concentrations were normalized to *Actb* mRNA. *$P < 0.05$, **$P < 0.01$, ***$P < 0.001$, and ****$P < 0.0001$. E18.5 = 18.5 days after coitum.

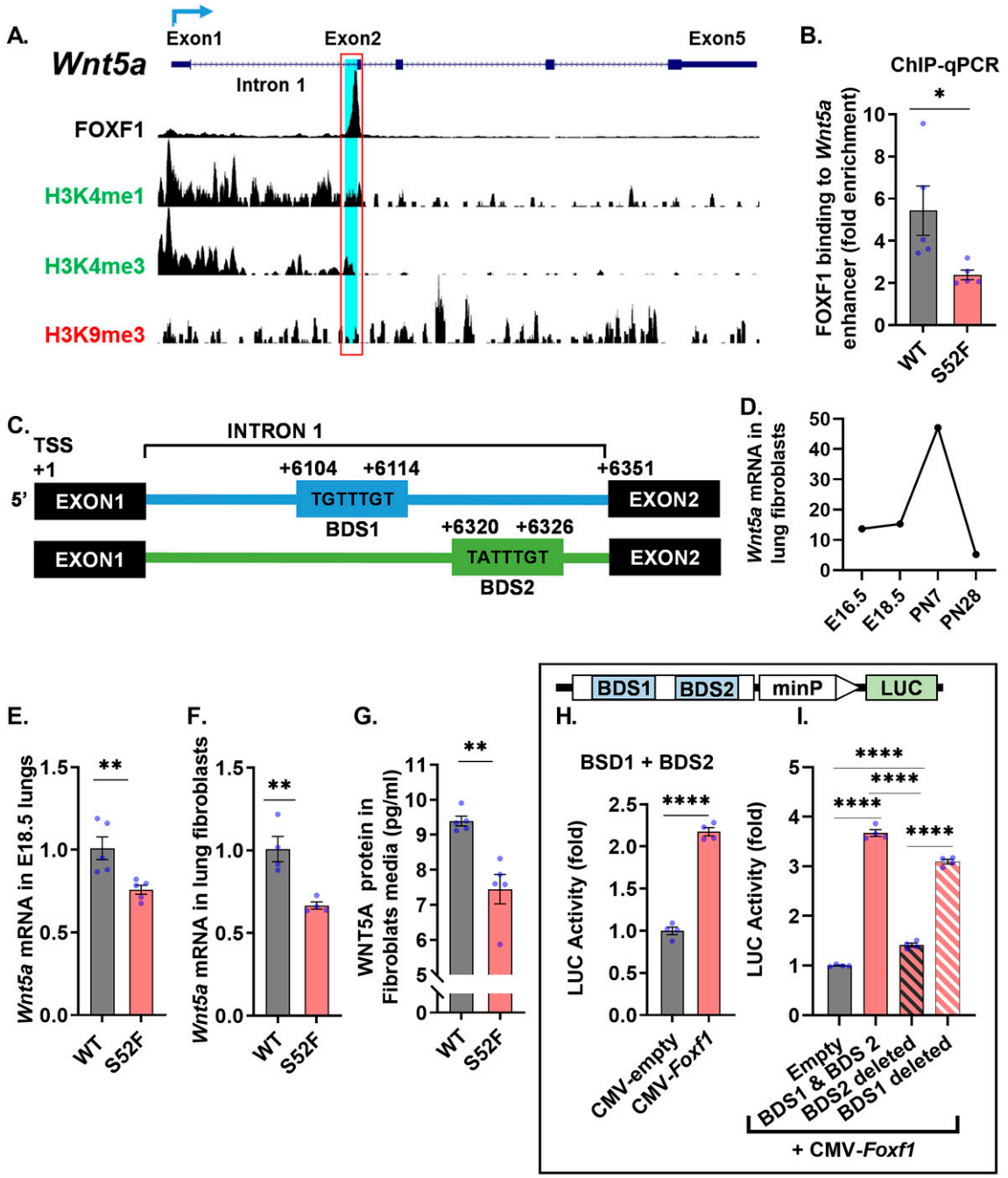

Figure 6. FOXF1 stimulates *Wnt5a* (Wnt family member 5A) gene expression through the +6320/+6326 *Wnt5a* DNA region. (*A*) FOXF1 Chromatin Immunoprecipitation Sequencing (ChIP-seq) was performed using WT E18.5 mouse lungs. FOXF1-binding region in the first intron of the mouse *Wnt5a* gene is shown with a red box. FOXF1 ChIP-seq data were aligned with ChIP-seq data sets showing histone modifications favoring gene transcription (H3K4me1, H3K4me3) or gene repression (H3K9me3). (*B*) ChIP-qPCR shows that *Foxf1*$^{WT/S52F}$ mouse lung fibroblasts exhibit decreased binding of FOXF1 protein to the *Wnt5a* enhancer compared with WT lung fibroblasts (control). Lung fibroblasts were isolated from individual mice ($n = 4$). (*C*) Schematic shows the location of two FOXF1 DNA-binding motifs in the first intron of the *Wnt5a* gene locus. (*D*) RNA sequencing shows that *Wnt5a* mRNA is present in the lung tissue at different stages of lung development. Data were obtained from single-cell data sets of mouse WT lungs available from LungMAP (https://lungmap.net). (*E*) qRT-PCR shows that *Wnt5a* mRNA is decreased in total lung RNA from *Foxf1*$^{WT/S52F}$ E18.5 embryos ($n = 4$ lungs per group). (*F*) *Wnt5a* mRNA is lower in primary lung fibroblasts obtained from *Foxf1*$^{WT/S52F}$ mice compared with WT littermates. Fibroblasts were isolated from individual mice ($n = 4$ mice per group). qRT-PCR data were normalized to *Actb* mRNA. (*G*) ELISA shows decreased concentrations of WNT5A protein in conditioned media from *Foxf1*$^{WT/S52F}$ lung fibroblasts compared with WT lung fibroblasts ($n = 4$ mice per group). (*H* and *I*) Dual-luciferase assay shows that the +6320/+6326 FOXF1-binding site (BDS2) is required for the activation of the *Wnt5a* enhancer ($n = 4$). Deletion of BDS1 site had no effect. LUC reporter plasmids were cotransfected with either cytomegalovirus (CMV)–*Foxf1* or CMV–empty plasmids using 293T cells. *$P < 0.05$, **$P < 0.01$, and ****$P < 0.0001$. BDS = binding site; minP = minimal promoter; PN = postnatal day; qPCR = quantitative PCR; TSS = transcription start site.

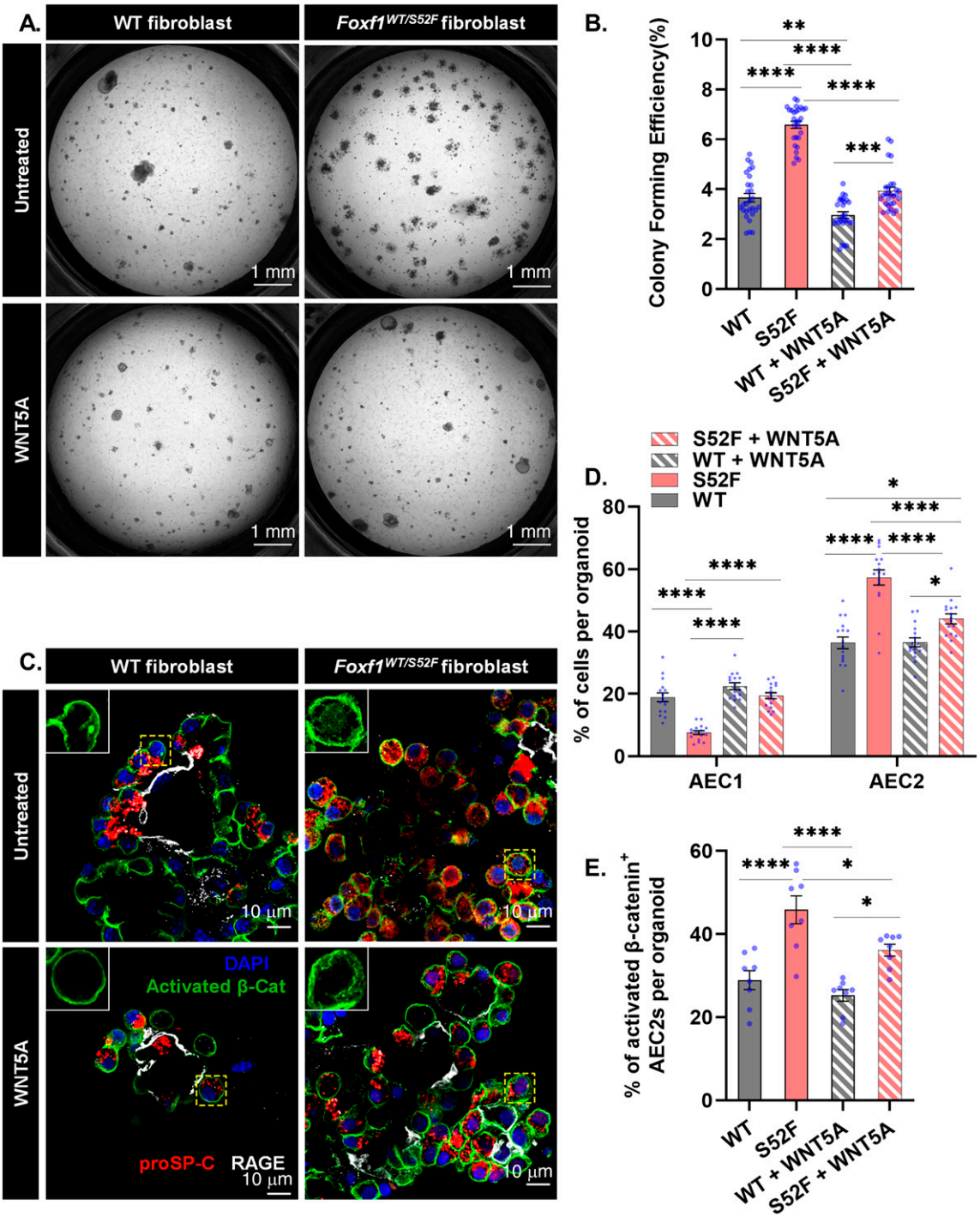

Figure 7. Treatment with exogenous WNT5A mitigates the effects of the *S52F Foxf1* mutation in alveolar organoids. (*A*) Images of lung organoids show that WNT5A treatment decreases the number and size of lung organoids containing *Foxf1*$^{WT/S52F}$ fibroblasts and WT epithelial cells. Organoids containing WT fibroblasts and WT epithelial cells were used as controls. Scale bars, 1 mm. (*B*) The colony-forming efficiency of lung organoids containing *Foxf1*$^{WT/S52F}$ fibroblasts is decreased after WNT5A treatment ($n = 28$ wells). (*C*) Immunostaining for proSP-C (red), RAGE (white), and activated phospho-β-catenin (green) shows AEC2s with activated β-catenin in WT and mutant organoids after treatment with WNT5A. Cell nuclei were counterstained with DAPI (blue). Scale bars, 10 μm. (*D*) WNT5A treatment decreases the percentage of AEC2s and increases the percentage of AEC1s in *Foxf1*$^{WT/S52F}$ organoids compared with untreated *Foxf1*$^{WT/S52F}$ organoids ($n = 16$). Cells were counted using high-magnification confocal images. (*E*) The number of AEC2s with activated β-catenin is decreased in *Foxf1*$^{WT/S52F}$ organoids after WNT5A treatment ($n = 8$). $^{*}P < 0.05$, $^{**}P < 0.01$, $^{***}P < 0.001$, $^{****}P < 0.0001$. Cat = catenin.

in mammals (*see* Figure E11) and contains two FOXF1-binding motifs (binding site 1 [BDS1] and BDS2) that are located on opposite strands of DNA (Figure 6C). BDS1 is located at position +6104/+6114 from the transcription start site on the coding DNA strand, whereas BDS2 resides on the template strand at +6320/+6326 from the transcription start site.

Analysis of single-cell RNA sequencing data from mouse lungs in the LungMAP web portal (https://lungmap.net) showed that *Wnt5a* is expressed in lung fibroblasts during embryonic and postnatal lung development but is decreased in the adult lung (Figure 6D). Mesenchymal cells were the highest *Wnt5a* mRNA-expressing cell type in E18.5 WT lungs (*see* Figure E12A). *Wnt5a* mRNA was decreased in E18.5 *Foxf1*$^{WT/S52F}$ lung tissue compared with WT lungs, as shown by qRT-PCR of total lung RNA (Figure 6E) and by RNAScope for *Wnt5a* and *Vim* mRNAs (*see* Figures E12B and E12C). Furthermore, *Wnt5a* mRNA expression was lower in purified *Foxf1*$^{WT/S52F}$ fibroblasts compared with WT fibroblasts (Figure 6F). The concentration of WNT5A protein was also lower in conditioned media from *Foxf1*$^{WT/S52F}$ fibroblasts, as shown by ELISA (Figure 6G). Thus, the *S52F Foxf1* mutation decreases the expression of *Wnt5a* in lung fibroblasts. To determine if FOXF1 directly activates the *Wnt5a* enhancer, we constructed several LUC reporter plasmids in which the *Wnt5a* intronic enhancer or its mutants were cloned together with the minimal promoter driving LUC expression (*see* Figures E13A–E13C). Dual-LUC assay demonstrated that the CMV–*Foxf1* expression vector stimulates the activity of the *Wnt5a* enhancer in cotransfection experiments (Figure 6H). Site-directed mutagenesis of the BDS2 FOXF1 motif almost completely inhibited the transcriptional activity of the *Wnt5a* enhancer, whereas disruption of the BDS1 FOXF1-binding motif had no effect (Figure 6I). These results demonstrate that FOXF1 directly activates the *Wnt5a* intronic enhancer through the +6320/+6326 BDS2 region.

Treatment of Lung Organoids with Exogenous WNT5A Alleviates the Effects of the *S52F Foxf1* Mutation on Epithelial Differentiation and Canonical WNT Signaling

Having established that FOXF1 stimulates *Wnt5a* gene expression and that WNT5A is reduced in *Foxf1*$^{WT/S52F}$ fibroblasts, we tested whether treating lung organoids with recombinant WNT5A will decrease the effects of *S52F Foxf1* mutation on epithelial proliferation. Treatment with WNT5A reduced the colony-forming efficiency of *Foxf1*$^{WT/S52F}$ fibroblasts to the degrees seen in untreated WT controls (Figures 7A and 7B). Furthermore, the numbers of large, medium, and small *Foxf1*$^{WT/S52F}$ organoids were decreased after treatment with WNT5A (*see* Figures E14A and E14B). Interestingly, WT organoids were less responsive to exogenous WNT5A (Figures 7A and 7B and E14A and E14B), probably because of high endogenous WNT5A expression (Figures 6F and 6G). However, WT organoids were sensitive to depletion of WNT5A through the antibody treatment (*see* Figure E15A); treatment of WT organoids with WNT5A-blocking antibody increased the size of the organoids and the colony-forming efficiency (*see* Figures E15B and E15C).

Next, we examined epithelial differentiation in WNT5A-treated lung organoids. WNT5A treatment prevented an aberrant increase of AEC2 numbers in the *Foxf1*$^{WT/S52F}$ mutant organoids, as demonstrated by immunostaining for proSP-C (Figures 7C and 7D) and qRT-PCR for *Sftpc* mRNA (*see* Figure E16A). Furthermore, WNT5A treatment restored the number of AEC1s (Figures 7C and 7D) and increased *Aqp5* and *Ager* mRNAs in the *Foxf1*$^{WT/S52F}$ mutant organoids (*see* Figures E16B and E16C). Thus, exogenous WNT5A restores the epithelial differentiation in alveolar organoids with *Foxf1*$^{WT/S52F}$ fibroblasts.

As WNT5A is a noncanonical WNT ligand and inhibits the canonical WNT/β-catenin signaling pathway in lung epithelial cells *in vitro* and *in vivo* (43, 44), we examined the expression of activated phospho-β-catenin in AEC2s after treatment of lung organoids with exogenous WNT5A. The percentage of AEC2s with nuclear β-catenin was decreased after treating the *Foxf1*$^{WT/S52F}$ organoids with WNT5A (Figures 7C and 7E). Decreased activation of β-catenin in WNT5A-treated AEC2s was associated with reduced expression of WNT/β-catenin downstream target genes as demonstrated by immunostaining for cyclinD1 (*see* Figure E16D) and qRT-PCR for *Ccnd1*, *Fzd1*, and *Axin2* mRNAs (*see* Figures E16E–E16G). Interestingly, treatment of WT organoids with WNT5A-blocking antibody increased canonical WNT/β-catenin signaling, as shown by increased numbers of AEC2s with activated β-catenin (*see* Figures E17A and E17B). Altogether, our results demonstrate that exogenous WNT5A alleviates the effects of the *S52F Foxf1*$^{WT/S52F}$ mutation on organoid growth and alveolar epithelial differentiation by inhibiting aberrant WNT/β-catenin signaling in AEC2s.

Discussion

Mesenchymal–epithelial cross-talk is essential for lung development and lung repair after injury in various respiratory diseases, including asthma, idiopathic pulmonary fibrosis, acute respiratory distress syndrome, and chronic obstructive pulmonary disease (1–4, 14, 28). In this study, we investigated the influence of fibroblast cells on the maintenance and proliferation of alveolar epithelial cells using an organoid system. AEC2s act as alveolar epithelial progenitor cells that self-renew and differentiate into AEC1s (2, 3). Published studies demonstrated that canonical WNT/β-catenin signaling is required for the maintenance and proliferation of alveolar epithelial progenitors (3, 8, 9). Overexpression of activated β-catenin in airway club cells leads to ectopic expansion of alveolar epithelial cells into the airway compartment (9). Lineage-tracing experiments with *Sftpc*^{CreERT2}; *Ctnnb1*$^{fl(Ex3)/+}$ mice showed that WNT/β-catenin signaling promotes clonal expansion of AEC2s (45). In contrast, inhibition of WNT/β-catenin signaling prevents the expansion of AEC2s and promotes AEC2 differentiation toward the AEC1 lineage. Treatment of lung alveolar organoids with canonical WNT3A ligand increases organoid formation (45). Consistent with published studies, we found increased activation of WNT/β-catenin signaling in AEC2s of alveolar organoids grown in the presence of FOXF1-deficient fibroblasts, as evident by increased organoid growth, increased numbers of AEC2s with nuclear β-catenin and elevated expression of transcriptional targets of the canonical WNT/β-catenin signaling pathway. As the *S52F Foxf1* mutant is transcriptionally inactive (12), our findings suggest that FOXF1 deficiency in lung fibroblasts stimulates canonical WNT/β-catenin signaling in AEC2s. It is possible that the *Foxf1*$^{WT/S52F}$ mutation in lung fibroblasts accelerates the expansion of AEC2s or prevents differentiation of AEC2s into AEC1s in lung organoids (7). Our results are

consistent with those of published studies demonstrating that FOXF1-deficient mice develop intestinal hyperplasia because of activation of canonical WNT/β-catenin signaling in intestinal epithelial cells (46).

Both canonical and noncanonical WNT signaling pathways have been implicated in the regulation of AEC2 differentiation (2, 3). In contrast to the canonical WNT pathway, which leads to the translocation of β-catenin to the nucleus to regulate gene expression as a coactivator of TCF (T-cell factor)/LEF (lymphoid enhancer factor) transcription factors, noncanonical WNT pathways do not depend on β-catenin but involve other intracellular mechanisms (3). In most cases, noncanonical WNT pathways repress canonical WNT/β-catenin signaling (2, 3). WNT5A is one of the most studied noncanonical WNTs, produced mostly by mesenchyme to regulate epithelial morphogenesis during lung development. Although WNT5A is also produced by other respiratory cell types, including epithelial cells, WNT5a expression in nonmesenchymal cells is lower. WNT5A requires the ROR coreceptor on the surface of epithelial cells to regulate canonical WNT/β-catenin signaling (47); however, other mechanisms can contribute to the regulation of canonical WNT signaling by WNT5A. Deletion of *Wnt5a* in the mouse results in truncation of the trachea, expansion of the distal airway compartment, and lung immaturity because of reduced differentiation of AEC1s from distal epithelial progenitors (7). In contrast, overexpression of *Wnt5a* yields opposite phenotypes. *Wnt5a*-overexpressing mice exhibit reduced epithelial branching and the early onset of lung maturation because of increased differentiation of AEC1s (48). Similar findings were observed after overexpression of WNT5A in developing chick embryos (49). Recently, it was reported that WNT5A and WNT5B can both inhibit and activate the canonical WNT/β-catenin signaling pathway in epithelial cells (43, 50). Canonical WNT/β-catenin signaling in alveolar epithelial cells was suppressed by fibroblast-derived WNT5A *in vitro* and *in vivo* (44), suggesting a balance between activating and repressing effects of WNT5A on canonical WNT/β-catenin signaling that can depend on the timing of lung development or the cellular niche. Our WNT5A rescue experiments are consistent with the inhibitory effect of WNT5A on WNT/β-catenin signaling and demonstrate that treating alveolar organoids with exogenous WNT5A reduces the number of AEC2s with nuclear β-catenin, decreases AEC2 proliferation, and increases the differentiation of AEC1s. WNT5A inhibits aberrant canonical WNT/β-catenin signaling in AEC2s caused by coculture of epithelial cells with *Foxf1*$^{WT/S52F}$ fibroblasts (*see* Figure E18). As FOXF1 transcriptionally activates *Wnt5a*, decreased expression of *Wnt5a* in *S52F Foxf1* mutant fibroblasts and *Foxf1*$^{WT/S52F}$ mice can be a consequence of FOXF1 deficiency.

Consistent with our organoid data, *Foxf1*$^{WT/S52F}$ lungs exhibited increased proliferation of AEC2s and decreased AEC1 differentiation. It is likely that loss of AEC1s contributes to respiratory distress in *Foxf1*$^{WT/S52F}$ mice because of reduced surface area available for gas exchange. A decrease in AEC1s was also reported in infants with ACDMPV, who experience severe breathing problems and diminished oxygenation in the peripheral blood (2). On the basis of our observations in lung organoids and *Foxf1*$^{WT/S52F}$ lungs, it is possible that FOXF1-mediated regulation of *Wnt5a* in lung fibroblasts plays a critical role in alveolarization by ensuring proper differentiation of alveolar epithelial cell lineages. Although we found that the *Foxf1*$^{WT/S52F}$ mutation did not influence fibroblast proliferation in cell culture conditions, it is possible that this mutation can cause intrinsic abnormalities in lung fibroblasts, such as diminished cell migration or altered ECM production, leading to impaired alveolarization independently of the impact of this mutation on WNT5A and mesenchymal–epithelial cross-talk. Consistent with this hypothesis, FOXF1 transcriptionally regulates multiple mesenchymal genes critical for cell migration and ECM production (2, 12, 13).

Conclusions

FOXF1 stimulates *Wnt5a* gene expression through the +6320/+6326 *Wnt5a* enhancer, maintaining an appropriate concentration of Wnt5a in lung fibroblasts. FOXF1-mediated activation of *Wnt5a* is essential for epithelial morphogenesis by inhibiting canonical WNT/β-catenin signaling in AEC2s and stimulating differentiation of AEC1s. Pharmacological activation of either FOXF1 or WNT5A may provide an attractive strategy to improve respiratory outcomes in patients with ACDMPV. ■

Author disclosures are available with the text of this article at www.atsjournals.org.

References

1. Bolte C, Whitsett JA, Kalin TV, Kalinichenko VV. Transcription factors regulating embryonic development of pulmonary vasculature. *Adv Anat Embryol Cell Biol* 2018;228:1–20.
2. Whitsett JA, Kalin TV, Xu Y, Kalinichenko VV. Building and regenerating the lung cell by cell. *Physiol Rev* 2019;99:513–554.
3. Morrisey EE, Hogan BL. Preparing for the first breath: genetic and cellular mechanisms in lung development. *Dev Cell* 2010;18:8–23.
4. McCulley D, Wienhold M, Sun X. The pulmonary mesenchyme directs lung development. *Curr Opin Genet Dev* 2015;32:98–105.
5. Bolte C, Kalin TV, Kalinichenko VV. Molecular, cellular, and bioengineering approaches to stimulate lung regeneration after injury. *Semin Cell Dev Biol* 2020;100:101–108.
6. Aros CJ, Pantoja CJ, Gomperts BN. Wnt signaling in lung development, regeneration, and disease progression. *Commun Biol* 2021;4:601.
7. Li C, Xiao J, Hormi K, Borok Z, Minoo P. Wnt5a participates in distal lung morphogenesis. *Dev Biol* 2002;248:68–81.
8. Mucenski ML, Wert SE, Nation JM, Loudy DE, Huelsken J, Birchmeier W, *et al.* β-Catenin is required for specification of proximal/distal cell fate during lung morphogenesis. *J Biol Chem* 2003; 278:40231–40238.
9. Mucenski ML, Nation JM, Thitoff AR, Besnard V, Xu Y, Wert SE, *et al.* Beta-catenin regulates differentiation of respiratory epithelial cells in vivo. *Am J Physiol Lung Cell Mol Physiol* 2005;289:L971–L979.
10. Nasr T, Holderbaum AM, Chaturvedi P, Agarwal K, Kinney JL, Daniels K, *et al.* Disruption of a hedgehog-foxf1-rspo2 signaling axis leads to tracheomalacia and a loss of sox9+ tracheal chondrocytes. *Dis Model Mech* 2020;14:dmm046573.
11. Dharmadhikari AV, Szafranski P, Kalinichenko VV, Stankiewicz P. Genomic and epigenetic complexity of the foxf1 locus in 16q24.1: implications for development and disease. *Curr Genomics* 2015;16: 107–116.
12. Pradhan A, Dunn A, Ustiyan V, Bolte C, Wang G, Whitsett JA, *et al.* The s52f foxf1 mutation inhibits stat3 signaling and causes alveolar capillary dysplasia. *Am J Respir Crit Care Med* 2019;200: 1045–1056.

13. Ustiyan V, Bolte C, Zhang Y, Han L, Xu Y, Yutzey KE, *et al.* FOXF1 transcription factor promotes lung morphogenesis by inducing cellular proliferation in fetal lung mesenchyme. *Dev Biol* 2018;443:50–63.
14. Black M, Milewski D, Le T, Ren X, Xu Y, Kalinichenko VV, *et al.* Foxf1 inhibits pulmonary fibrosis by preventing cdh2-cdh11 cadherin switch in myofibroblasts. *Cell Rep* 2018;23:442–458.
15. Kalinichenko VV, Gusarova GA, Shin B, Costa RH. The forkhead box F1 transcription factor is expressed in brain and head mesenchyme during mouse embryonic development. *Gene Expr Patterns* 2003;3:153–158.
16. Kalinichenko VV, Zhou Y, Shin B, Stolz DB, Watkins SC, Whitsett JA, *et al.* Wild-type levels of the mouse Forkhead Box f1 gene are essential for lung repair. *Am J Physiol Lung Cell Mol Physiol* 2002;282: L1253–L1265.
17. Kolesnichenko OA, Whitsett JA, Kalin TV, Kalinichenko VV. Therapeutic potential of endothelial progenitor cells in pulmonary diseases. *Am J Respir Cell Mol Biol* 2021;65:473–488.
18. Cai Y, Bolte C, Le T, Goda C, Xu Y, Kalin TV, *et al.* FOXF1 maintains endothelial barrier function and prevents edema after lung injury. *Sci Signal* 2016;9:ra40.
19. Kalin TV, Meliton L, Meliton AY, Zhu X, Whitsett JA, Kalinichenko VV. Pulmonary mastocytosis and enhanced lung inflammation in mice heterozygous null for the Foxf1 gene. *Am J Respir Cell Mol Biol* 2008; 39:390–399.
20. Mahlapuu M, Ormestad M, Enerbäck S, Carlsson P. The forkhead transcription factor Foxf1 is required for differentiation of extra-embryonic and lateral plate mesoderm. *Development* 2001;128:155–166.
21. Lim L, Kalinichenko VV, Whitsett JA, Costa RH. Fusion of lung lobes and vessels in mouse embryos heterozygous for the forkhead box f1 targeted allele. *Am J Physiol Lung Cell Mol Physiol* 2002;282: L1012–L1022.
22. Wang G, Wen B, Deng Z, Zhang Y, Kolesnichenko OA, Ustiyan V, *et al.* Endothelial progenitor cells stimulate neonatal lung angiogenesis through FOXF1-mediated activation of BMP9/ACVRL1 signaling. *Nat Commun* 2022;13:2080.
23. Ren X, Ustiyan V, Guo M, Wang G, Bolte C, Zhang Y, *et al.* Postnatal alveologenesis depends on foxf1 signaling in c-kit(+) endothelial progenitor cells. *Am J Respir Crit Care Med* 2019;200:1164–1176.
24. Barkauskas CE, Chung MI, Fioret B, Gao X, Katsura H, Hogan BL. Lung organoids: current uses and future promise. *Development* 2017;144: 986–997.
25. Gkatzis K, Taghizadeh S, Huh D, Stainier DYR, Bellusci S. Use of three-dimensional organoids and lung-on-a-chip methods to study lung development, regeneration and disease. *Eur Respir J* 2018;52:1800876.
26. Sun F, Wang G, Pradhan A, Xu K, Gomez-Arroyo J, Zhang Y, *et al.* Nanoparticle delivery of stat3 alleviates pulmonary hypertension in a mouse model of alveolar capillary dysplasia. *Circulation* 2021;144: 539–555.
27. Kim IM, Zhou Y, Ramakrishna S, Hughes DE, Solway J, Costa RH, *et al.* Functional characterization of evolutionarily conserved DNA regions in forkhead box f1 gene locus. *J Biol Chem* 2005;280: 37908–37916.
28. Sun L, Ren X, Wang IC, Pradhan A, Zhang Y, Flood HM, *et al.* The FOXM1 inhibitor RCM-1 suppresses goblet cell metaplasia and prevents IL-13 and STAT6 signaling in allergen-exposed mice. *Sci Signal* 2017;10:eaai8583.
29. Ustiyan V, Wert SE, Ikegami M, Wang IC, Kalin TV, Whitsett JA, *et al.* Foxm1 transcription factor is critical for proliferation and differentiation of Clara cells during development of conducting airways. *Dev Biol* 2012;370:198–212.
30. Bolte C, Zhang Y, Wang IC, Kalin TV, Molkentin JD, Kalinichenko VV. Expression of Foxm1 transcription factor in cardiomyocytes is required for myocardial development. *PLoS One* 2011;6:e22217.
31. Zacharias WJ, Frank DB, Zepp JA, Morley MP, Alkhaleel FA, Kong J, *et al.* Regeneration of the lung alveolus by an evolutionarily conserved epithelial progenitor. *Nature* 2018;555:251–255.
32. Xia H, Ren X, Bolte CS, Ustiyan V, Zhang Y, Shah TA, *et al.* Foxm1 regulates resolution of hyperoxic lung injury in newborns. *Am J Respir Cell Mol Biol* 2015;52:611–621.
33. Ustiyan V, Zhang Y, Perl AK, Whitsett JA, Kalin TV, Kalinichenko VV. β-Catenin and Kras/Foxm1 signaling pathway are critical to restrict Sox9 in basal cells during pulmonary branching morphogenesis. *Dev Dyn* 2016;245:590–604.
34. Wang X, Bhattacharyya D, Dennewitz MB, Kalinichenko VV, Zhou Y, Lepe R, *et al.* Rapid hepatocyte nuclear translocation of the forkhead box M1B (FoxM1B) transcription factor caused a transient increase in size of regenerating transgenic hepatocytes. *Gene Expr* 2003;11: 149–162.
35. Dunn AW, Kalinichenko VV, Shi D. Highly efficient in vivo targeting of the pulmonary endothelium using novel modifications of polyethylenimine: an importance of charge. *Adv Healthc Mater* 2018;7:e1800876.
36. Bolte C, Ustiyan V, Ren X, Dunn AW, Pradhan A, Wang G, *et al.* Nanoparticle delivery of proangiogenic transcription factors into the neonatal circulation inhibits alveolar simplification caused by hyperoxia. *Am J Respir Crit Care Med* 2020;202:100–111.
37. Ren X, Zhang Y, Snyder J, Cross ER, Shah TA, Kalin TV, *et al.* Forkhead box M1 transcription factor is required for macrophage recruitment during liver repair. *Mol Cell Biol* 2010;30:5381–5393.
38. Milewski D, Balli D, Ustiyan V, Le T, Dienemann H, Warth A, *et al.* FOXM1 activates AGR2 and causes progression of lung adenomas into invasive mucinous adenocarcinomas. *PLoS Genet* 2017;13: e1007097.
39. Dharmadhikari AV, Sun JJ, Gogolewski K, Carofino BL, Ustiyan V, Hill M, *et al.* Lethal lung hypoplasia and vascular defects in mice with conditional Foxf1 overexpression. *Biol Open* 2016;5: 1595–1606.
40. Bolte C, Flood HM, Ren X, Jagannathan S, Barski A, Kalin TV, *et al.* FOXF1 transcription factor promotes lung regeneration after partial pneumonectomy. *Sci Rep* 2017;7:10690.
41. Bolte C, Ren X, Tomley T, Ustiyan V, Pradhan A, Hoggatt A, *et al.* Forkhead box F2 regulation of platelet-derived growth factor and myocardin/serum response factor signaling is essential for intestinal development. *J Biol Chem* 2015;290:7563–7575.
42. Hoggatt AM, Kim JR, Ustiyan V, Ren X, Kalin TV, Kalinichenko VV, *et al.* The transcription factor Foxf1 binds to serum response factor and myocardin to regulate gene transcription in visceral smooth muscle cells. *J Biol Chem* 2013;288:28477–28487.
43. Wu X, van Dijk EM, Ng-Blichfeldt JP, Bos IST, Ciminieri C, Königshoff M, *et al.* Mesenchymal wnt-5a/5b signaling represses lung alveolar epithelial progenitors. *Cells* 2019;8:1147.
44. Baarsma H, Königshoff M. Wnt5a antagonizes canonical WNT/β-catenin signaling in lung epithelial cells. *Eur Respir J* 2013;42:4893.
45. Frank DB, Peng T, Zepp JA, Snitow M, Vincent TL, Penkala IJ, *et al.* Emergence of a wave of wnt signaling that regulates lung alveologenesis by controlling epithelial self-renewal and differentiation. *Cell Rep* 2016;17:2312–2325.
46. Ormestad M, Astorga J, Landgren H, Wang T, Johansson BR, Miura N, *et al.* Foxf1 and Foxf2 control murine gut development by limiting mesenchymal Wnt signaling and promoting extracellular matrix production. *Development* 2006;133:833–843.
47. Kumawat K, Gosens R. WNT-5A: signaling and functions in health and disease. *Cell Mol Life Sci* 2016;73:567–587.
48. Li C, Hu L, Xiao J, Chen H, Li JT, Bellusci S, *et al.* Wnt5a regulates Shh and Fgf10 signaling during lung development. *Dev Biol* 2005;287: 86–97.
49. Loscertales M, Mikels AJ, Hu JK, Donahoe PK, Roberts DJ. Chick pulmonary Wnt5a directs airway and vascular tubulogenesis. *Development* 2008;135:1365–1376.
50. Nabhan AN, Brownfield DG, Harbury PB, Krasnow MA, Desai TJ. Single-cell Wnt signaling niches maintain stemness of alveolar type 2 cells. *Science* 2018;359:1118–1123.